RESEARCH ARTICLE

Proteomic analysis of estrogen response of premalignant human breast cells using a 2-D liquid separation/mass mapping technique

Jia Zhao[1], Kan Zhu[1], David M. Lubman[1, 2, 3], Fred R. Miller[4, 5], Malthy P. V. Shekhar[4, 5], Brigitte Gerard[4] and Timothy J. Barder[6]

[1] Department of Chemistry, University of Michigan, Ann Arbor, MI, USA
[2] Department of Surgery, University of Michigan Medical Center, Ann Arbor, MI, USA
[3] Comprehensive Cancer Center, University of Michigan Medical Center, Ann Arbor, MI, USA
[4] Breast Cancer Program, Barbara Ann Karmanos Cancer Institute, Detroit, MI, USA
[5] Department of Pathology, Wayne State University School of Medicine, Detroit, MI, USA
[6] Eprogen, Darien, IL, USA

A 2-D liquid-phase separation method based on chromatofocusing and nonporous silica RP-HPLC followed by ESI-TOF-MS was used to analyze proteins in whole cell lysates from estrogen-treated and untreated premalignant, estrogen-responsive cell line MCF10AT1 cells. 2-D mass maps in the pH range 4.6–6.0 were generated with good correlation to theoretical M_r values for intact proteins. Proteins were identified based on intact M_r, p*I* and PMF, or MS/MS sequencing. About 300 unique proteins were identified and 120 proteins in mass range 5–75 kDa were quantified upon treatment of estrogen. Around 40 proteins were found to be more highly expressed (>four-fold) and 17 were down-regulated (>four-fold) in treated cells. In our study, we found that many altered proteins have characteristics consistent with the development of a malignant phenotype. Some of them have a role in the ras pathway or play an important role in signal pathways. These changed proteins might be essential in the estrogen regulation mechanism. Our study highlights the use of the MCF10AT1 cell line to examine estrogen-induced changes in premalignant breast cells and the ability of the 2-D mass mapping technique to quantitatively study protein expression changes on a proteomic scale.

Received: March 31, 2005
Revised: January 29, 2006
Accepted: February 7, 2006

Keywords:
Biomarker / Breast cancer / Liquid chromatography / Mass spectrometry

1 Introduction

Breast carcinoma is the second leading cause of cancer-related death in women in the Western world [1]. Despite significant improvements in cancer diagnosis and treatment, 40 000 women are expected to die from the disease this year [2]. The effect of ovarian hormones such as estrogen on breast cancer risk was first shown over 100 years ago when researchers found that removing the ovaries of women with breast cancer improved their chances of survival. Furthermore, lifetime exposure to estrogen is associated with increasing a woman's risk for breast cancer [3, 4].

The growth of breast cancer cells is under the control of estrogenic hormones and growth factors [5]. Estrogen is a hormone that is essential for the normal growth and development of the breast and tissues important for sexual reproduction. Estrogen is produced by the ovaries and aromatase-expressing cells peripheral to the ovaries. It is recognized and used in estrogen target tissues with estrogen recep-

Correspondence: Dr. David M. Lubman, Department of Surgery, The University of Michigan Medical Center, MSRB1, 1150 West Medical Center Drive, Ann Arbor, MI 48109-0656, USA
E-mail: dmlubman@umich.edu
Fax: +1-734-615-8108

Abbreviations: CF, chromatofocusing; **E2**, estradiol; **ER**, estrogen receptors; **NPS**, nonporous silica; ***n***-OG, *n*-octyl-β-D-glucopyranoside

tors (ER) such as the breast and uterus. The ER enters the nucleus and turns on the estrogen-responsive genes, which stimulate cell division. The progression from a normal cell to a cancer cell is a multi-step process that includes the build-up of damage to the DNA in key genes that control cell division and proliferation. Because estrogen stimulates cell division, it can enhance a spontaneous or chemically induced mutation. It can also indirectly stimulate cell division in the breast by affecting the level of other hormone receptors or growth factors [6].

To follow changes in cancer cells at the molecular level, the most commonly used method is to monitor the activation of different genes *via* mRNA expression as the cancer evolves. In order to gain accurate quantitation of gene expression levels in cells or tissues, DNA microarray techniques have been developed. The drawback of these techniques is that the correlation between mRNA and protein levels has been insufficient to predict protein expression levels from quantitative mRNA data [7]. In addition, genomic analysis provides the predicted sequence of proteins rather than the functional form found in the cell. A cell is normally dependent upon a multitude of metabolic and regulatory pathways for its survival. Proteomics is complementary to genomics because it focuses on the gene products, which are the active agents in cells. In addition, the number of protein isoforms expressed by a cell can be ten-fold higher than the number of coding genes where various protein modifications exist. Global protein profiling becomes the approach to address the complexity and changes in expression, including PTMs, during tumorigenesis. Proteomic analysis has been used widely in finding candidate biomarkers for early detection of cancer [8, 9].

Estrogen-induced changes are typically examined using human breast cancer MCF-7 cells. The MCF-7 line has been useful to study estrogen response and to develop selective ER modifiers such as tamoxifen [10] for breast cancer treatment. Because it expresses the ER, MCF-7 is often regarded as an early stage cancer and a model for examining altered estrogen response during progression. However, MCF-7 cells were derived from a malignant pleural effusion, which developed after treatment of two previous recurrences that occurred over a 3-year period. MCF-7 cells are aneuploid, nearly tetraploid, with a mean chromosomal number of 85 [11] and a DNA index of 1.7 [12]. Thus, MCF-7 is a poor model to test for alterations in early development of cancer from premalignant lesions. We have used the premalignant, estrogen-responsive cell line MCF10AT1 to examine the estrogen-induced changes in the proteome.

In order to study the estrogen-induced proteome, a novel CF-nonporous silica (NPS)-RP-HPLC-online-ESI-TOF-MS mass mapping approach is applied to analyze proteins from the premalignant human breast cell line before (MCF10AT1) and after treatment with estradiol (E2) (MCF10AT1E2) [13, 14]. In this study, the protein identification is based on PMF, MS/MS analysis, accurate MW, and p*I* of intact proteins. This method includes the fractionation of proteins based on p*I* in the first dimension using chromatofocusing (CF) and protein hydrophobicity in the second dimension using RP-HPLC which is followed by online ESI-TOF-MS detection. As a result, a 2-D mass map with p*I* in the first dimension and MW in the second dimension can be created. The abundance of proteins can be estimated by the peak area of the intact protein. The advantage of the method is that accurate p*I* and MW can be obtained for each protein. Moreover, since MS is a very specific detector, it can differentiate and quantify proteins that coelute. As a result, more proteins can be quantified with greater specificity compared to the 2-D UV map.

In this study, the protein identification is based on PMF, MS/MS analysis, accurate MW and p*I* of intact proteins. Proteins are identified by PMF using MALDI-TOF-MS or peptide sequencing using MALDI-TOF-TOF. The intact protein MW is obtained by ESI-TOF-MS in which M_r accurate to $<$150 ppm can be achieved. This method is essential for identifying the "exact" form of protein including information such as PTM, truncations, and isoforms of key proteins. The human breast epithelial cell line used in this study is premalignant in xenografts [15, 16]. The advantage of cell lines is the availability of a stable phenotype that can be modified after transfection with genes of interest. Since the MCF10AT1 can develop into xenograft lesions in different stages of cancer, it can truly mimic the progression of cancer. In this work, about 300 unique proteins are identified in the pH range studied (4.6–6.0) and around 120 high-abundance proteins are accurately quantified in the mass range 5–75 kDa. The 2-D mass maps and the corresponding protein identifications are valuable for proteomic analysis of cellular protein expression changes associated with E2 treatment. These proteins potentially play a role in the development of breast cancer.

2 Materials and methods

2.1 Cell culture

MCF10AT1 cells were grown in monolayer on plastic in DMEM/F12 medium (1:1 mixture of DMEM and Ham's F-12 medium) supplemented with 5% horse serum, 10 μg/mL of insulin, 20 ng/mL epidermal growth factor, and 0.5 μg/mL of hydrocortisone. MCF10AT1E2 lysates were prepared by treating ~50% confluent MCF10AT1 cell monolayers with 10^{-9} M E2 for 24 h. The cells were then collected by scraping and washed twice with PBS buffer before being stored at −70°C.

2.2 Cell lysis and buffer exchange

Approximately 70–80 million cells were thawed and lysed with five volumes of lysis buffer which consists of 7.5 M urea, 2.5 M thiourea, 4% *n*-octyl-β-D-glucopyranoside (*n*-OG), 10 mM tris(2-carboxyethyl)phosphine (TCEP), 12.5% v/v glycerol, and 1% v/v protease inhibitor cocktail

(Sigma, St. Louis, MO, USA). The mixture was vortexed frequently over a period of 1 h at room temperature and then centrifuged at 15 000 × *g* for 40 min at 4°C. After the supernatant was collected, buffer exchange was conducted against the CF start buffer using a PD-10 G-25 column (Amersham Biosciences, Piscataway, NJ, USA). The buffer-exchanged protein mixtures were stored in a −80°C freezer until further use. The Bradford assay [17] was used to quantify the amount of protein in mixtures.

2.3 CF

CF separation was performed on an HPCF-1D column (250 mm × 2.1 mm) (Beckman Coulter, Fullerton, CA, USA) using an ultra-plus II MD pump (Micro-tech Scientific, Vista, CA). Prior to sample loading, the column was equilibrated with a start buffer containing 25 mM bis-tris propane (Sigma), 6 M urea, and 1% *n*-OG. The pH of the start buffer was adjusted to pH 7.4 with saturated iminodiacetic acid solution. After equilibration, 4.5 mg of proteins were loaded onto the CF column. Elution is achieved by applying a pH 4.0 elution buffer that consists of 10% v/v Polybuffer 74 (Amersham Pharmacia, Piscataway, NJ), 6 M urea, and 1% *n*-OG at a flow rate of 0.2 mL/min. A linear pH gradient is generated at the outlet of the column. As a result, proteins elute off the column sequentially according to their p*I*. Separation is monitored at 280 nm using a UV detector. Accurate pH is measured online by a postdetector pH electrode/cell (Lazar Research Laboratories, Los Angeles, CA, USA) with low dead volume. Fractions were collected every 0.2 pH unit change from pH 7.0 to 4.0. Fractions of pH 6.0–4.6 were selected for further study due to the higher protein concentrations in these fractions.

2.4 NPS-RP-HPLC with sample collection

Following the CF fractionation, NPS-RP-HPLC is used to separate each fraction collected from the first dimension. High separation efficiency is achieved by using an ODSIII-E (4.6 mm × 33 mm) column (Eprogen, Darien, IL) packed with 1.5 μm nonporous silica. To collect purified proteins from NPS-RP-HPLC, the RP separation is performed at 0.5 mL/min and monitored at 214 nm using a Beckman 166 Model UV detector (Beckman-Coulter, Fullerton, CA, USA). Proteins eluting from the column were collected by an automated fraction collector (Model SC 100, Beckman), controlled by an in-house designed DOS-based software program. To enhance the speed, resolution, and reproducibility of the separation, the RP column is heated to 60°C by a column heater (Jones Chromatography, Model 7971). Both mobile phase A (water) and B (ACN) contains 0.1% v/v TFA. The gradient profile used is as follows: 5–15% B in 1 min, 15–25% B in 2 min, 25–31% B in 3 min, 31–41% B in 10 min, 41–47% B in 3 min, 47–67% B in 4 min, and 67–100% B in 1 min. Deionized water was purified using a Millipore RG system (Bedford, MA, USA).

2.5 NPS-RP-HPLC-online-ESI-TOF-MS

To map the proteins in the cell lysate, fractions obtained from CF were subject to NPS-RP-HPLC separation with online ESI-TOF-MS detection. The separation was performed under the same condition as in Section 2.4 except that 0.3% formic acid (Sigma) was added to both mobile phases to improve the ESI efficiency. The flow rate was maintained at 0.5 mL/min and a postcolumn splitter was used so that 200 μL/min was directed into an orthogonal acceleration ESI-TOF-MS (LCT; Micromass/Waters, Milford, MA, USA). The capillary voltage for electrospray was set at 3200 V, sample cone at 35 V, extraction cone at 3 V, and reflection lens at 750 V. Desolvation was accelerated by maintaining the desolvation temperature at 320°C and source temperature at 130°C. The desolvation gas flow was 650–800 L/h. One microgram bovine insulin (Sigma) was introduced to each sample as an internal standard. The intact molecular weight value was obtained by deconvoluting the combined ESI spectra with maximum entropy deconvolution algorithm (MaxEnt1) software.

2.6 Tryptic digestion

Each fraction obtained from NPS-RP-HPLC (Section 2.4) was concentrated down to ~20 μL with a SpeedVac concentrator (Labconco, Kansas City, MO) operating at 60°C. Twenty microliters of 100 mM ammonium bicarbonate (Sigma) was then mixed with each concentrated sample to obtain a pH value of about 7.8. About 0.5 μL of L-1-tosylamido-2-phenylethyl chloromethylketone (TPCK) modified sequencing-grade porcine trypsin (Promega, Madison, WI) was added and vortexed prior to a 20-h incubation at 37°C on an agitator.

2.7 MALDI sample preparation

Before MALDI analysis, each digested sample was desalted and concentrated to 5 μL using C18 ZipTip (Millipore). One microliter of the concentrated peptide mixture was spotted onto a Micromass 96-spot plate followed by 1 μL of matrix-standard layered on top of it. The MALDI matrix was prepared by diluting saturated α-CHCA (Sigma) solution with 50% v/v ACN and 1% v/v TFA at 1:4 ratio v/v. About 1 mg/mL angiotensin I (1296 Da), adrenocorticotropic hormone (ACTH clip 1–17, 2093 Da), and ACTH clip 18–39 (2465 Da) (Sigma) were diluted 100-fold with deionized water. These standards were further diluted 50, 40, and 30 times, respectively, with the diluted matrix.

2.8 PMF

In order to identify proteins in each fraction collected from NPS-RP-HPLC, MALDI-TOF-MS analysis was performed for each digested sample. With internal standards and delayed extraction reflectron TOF-MS (TOF Spec 2E, Micromass), a mass accuracy of less than 30 ppm can be consistently achieved. Monoisotopic masses of peptides were selected and searched against Swiss-Prot using MS-Fit http://prospector.

ucsf.edu/ucsfhtml4.0/msfit.htm. The following parameters were used in the search: (1) species: human; (2) maximum number of missed cleavage: 1; (3) possible modifications: peptide *N*-termal glutamine to pyro-glutamic acid, oxidation of methionine, and protein *N*-terminus acetylated; (4) peptide mass tolerance 50 ppm; (5) M_r of protein: 1000–100 000 Da; (6) p*I* range of protein 3–10. Only protein IDs with sequence coverage higher than 15% and MOWSE scores over 1000 were considered.

2.9 MALDI-TOF/TOF analysis of protein digests

To confirm the proteins identified by PMF and to identify proteins with low sequence coverage, MS/MS spectra were acquired for selected peptides using MALDI-TOF/TOF-MS (Q-Applied Biosystems, Foster City, CA, USA). About 0.5 μL aliquot of peptide solution was spotted on to an Applied Biosystems 192-spot plate covered by 0.5 μL matrix. According to the MALDI-TOF-MS data, eight peptides were selected from each spot for fragmentation. Collision energy was set at 1 kV. Ions with a mass window of ±4 Da were selected in the TOF/TOF timed ion selector. The MS/MS spectra was acquired and processed using 4700 Explorer. MASCOT was used to search the database. The parent ion mass tolerance was 60 ppm and the daughter ion mass tolerance was set to 0.3 Da. One missed cleavage was allowed and the possible modifications were *N*-acetyl, oxidation of methionine, phosphorylation of serine, threonine and tyrosine, and pyro-glu at *N*-term glutamine and glutamic acid.

2.10 Western blot analysis

Total cell lysates from MCF10AT1 and MCF10AT1E2 cells were prepared in 10 mM Tris-HCl, pH 7.5/150 mM NaCl/1% Triton X-100/1 mM PMSF, 1 μg/mL each of leupeptin, pepstatin, antipain, and 1 mM sodium orthovanadate. Proteins (50 μg) from each cell lysate were separated by SDS-PAGE and transblotted onto Immobilon P membranes. Steady-state levels of Grp75 were determined by reacting the membrane with anti-Grp75 mouse mAb (Abcam), and immunoreactive bands were visualized by chemiluminescence using ECL kit (Perkin Elmer). Equivalent aliquots of MCF10AT1 or MCF10AT1E2 protein fractions eluted from CF column (pH 4.6–6.0) were desalted and concentrated by filtration through Ultra free-MC 10K NMWL filter unit (Millipore), and subjected to SDS-PAGE and Western blot analysis of Grp75 as described above. Band intensities were quantitated with a Model 300A densitometer (Molecular Dynamics, Sunnyvale, CA).

3 Results and discussion

3.1 Cells

MCF10AT1 is derived from MCF10A by T-24 c-Ha-ras gene transfection. It is premalignant, but can develop into xenograft lesions spanning the spectrum from normal, atypical hyperplasia, ductal carcinoma *in situ* (DCIS), and invasive carcinomas. It truly represents early breast cancer progression since the human cell line MCF10A originated from spontaneous immortalization of breast epithelial cells obtained from a single patient with fibrocystic disease. Although E2 is not required for the formation and progression of MCF10AT1 lesions, it does accelerate progression in the xenografts formed [18]. The MCF10AT1 cells express ER (Erα) *in vitro* [19]. Thus, the analysis of proteins in MCF10AT1 and the E2-treated MCF10AT1E2 can reveal some key estrogen-regulated proteins which are involved in cancer progression.

3.2 Liquid-phase 2-D separation online ESI-TOF-MS analysis

Protein profiling techniques include 2-DE, liquid-phase IEF followed by RP separation online MS detection and the recently developed liquid 2-D separation based upon CF and RP separation, with UV detection. In this work, MCF10AT1 and MCF10AT1E2 cell lysates were separated with CF in the first dimension. The collected fractions were further separated by NPS-RP-HPLC and detected online using ESI-TOF-MS. The liquid-based method has the advantage of minimized sample handling, compatibility to MS analysis, improved recovery and reproducibility, improved resolution in the pH dimension, and fraction collection of proteins for further analysis. Online ESI-TOF-MS detection provides high mass accuracy, MW measurements, specificity, and accurate quantitation.

CF separates proteins according to the p*I*. It is a single chromatographic focusing procedure that combines the high capacity of ion-exchange chromatography with the high resolution of IEF. A typical CF chromatogram is shown in Fig. 1, where 4.7 mg cell extract from MCF10AT1E2 was fractionated. As shown, the change of pH at the outlet of column over time is linear from pH 7 to 4. In order to balance the resolution in the pH dimension and the number of fractions collected for further analysis, each fraction was collected with a 0.2 pH change. Over the course of a 60-min CF separation, a total of 15 fractions were obtained.

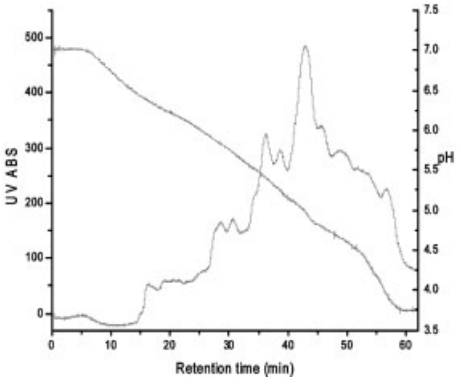

Figure 1. CF-UV chromatogram of 4.7 mg lysed AT1E2 cells. Flow rate = 0.2 mL/min. UV absorption was set at 280 nm.

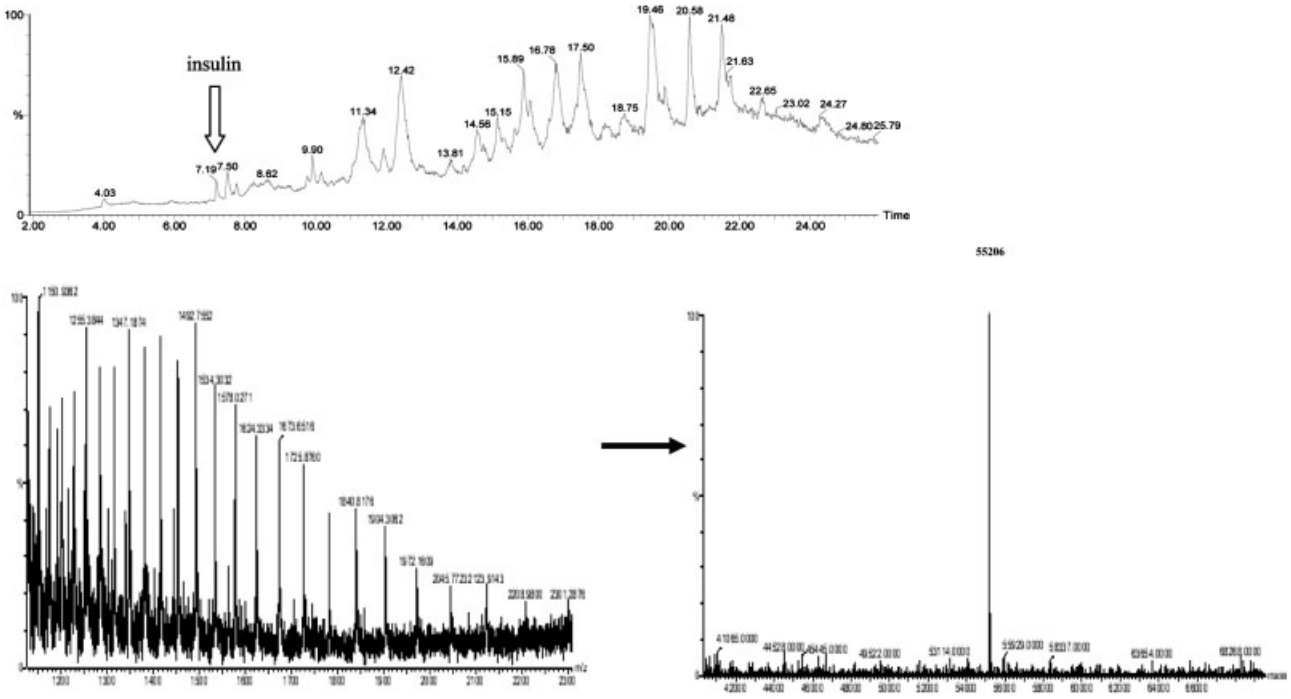

Figure 2. (a) NPS-RP-HPLC/ESI-MS-TIC chromatogram of CF fraction #8 (pH 5.4–5.2). One microgram bovine insulin was added as internal standard. (b) Combined mass spectra of the circled peak in Fig. 2a. MW was determined after deconvolution of a series of multiply charged ion peaks. This protein was identified as ATP synthase alpha chain. Experimental M_r (Exp. M_r = 55 206) matched the theoretical M_r of the truncated form (Theo. M_r = 55 209).

Fractions of pH 4.6–6.0 were further analyzed by NPS-RP-HPLC-online-ESI-TOF-MS. A total ion chromatogram of the LC-MS analysis for the MCF10AT1 fraction with pH 5.4–5.2 is shown in Fig. 2a. Proteins remain intact during the separation and MS analysis. During the 30 min separation, one spectrum is acquired *per* second. In order to obtain the MW of intact proteins, a series of multiply charged ion peaks in the combined spectrum (as shown in Fig. 2b) is deconvoluted. The theoretical mass of the protein, truncated ATP synthase alpha chain, is 55 209 Da. It is only 3 Da higher than the experimental MW of 55 206 Da, which suggests a mass accuracy of 50 ppm.

The abundance of each protein is indicated by the peak area of the deconvoluted peak of the intact protein. The entire amount of a protein present in each CF fraction can be obtained by deconvoluting the combined spectra of a selected ion chromatogram (SIC) created for the protein. To minimize the quantitation error induced by experimental variation, all peak areas obtained in a single LC-MS analysis were normalized to the deconvoluted peak area of insulin that was introduced as an internal standard.

3.3 2-D mass map

A mass map is created by integrating the MW, p*I*, and the abundance for all proteins in all CF fractions into one single image using ProteoVue or DeltaVue software. One such map is shown in Fig. 3a. The mass map resulted from the integration of the MW, p*I*, and abundance of all proteins in seven CF fractions with pH varying from 4.6 to 6.0. The map to the left is for MCF10AT1 cells, and the one to the right is for MCF10AT1E2 cells. In the visual 2-D map, the *y*-axis represents MW and *x*-axis represents pH. Each protein is shown as a band on the map with the intensity of the band indicating the abundance.

The 2-D map provides an overview of protein mass distribution and composition in each fraction in a pattern similar to 2-D PAGE. Moreover, differentially expressed proteins in the samples with and without estrogen treatment can be displayed, as shown in the middle of Fig. 3a. As a result, the complexity of a large number of proteins could be reduced to a virtual map and protein expression levels can be easily compared. The reproducibility of the protein profiling method is demonstrated in Fig. 4, where two differential maps of four CF fractions with pH 4.6–5.6 from two duplicate experiments are displayed.

3.4 Protein identification

From the CF-NPS-RP-HPLC online ESI-TOF-MS analysis, the MW, p*I*, and abundance information can be obtained. However, the protein identity is still unknown. Therefore, a separate NPS-RP-HPLC is conducted for each CF fraction using an identical gradient monitored by a UV detector and

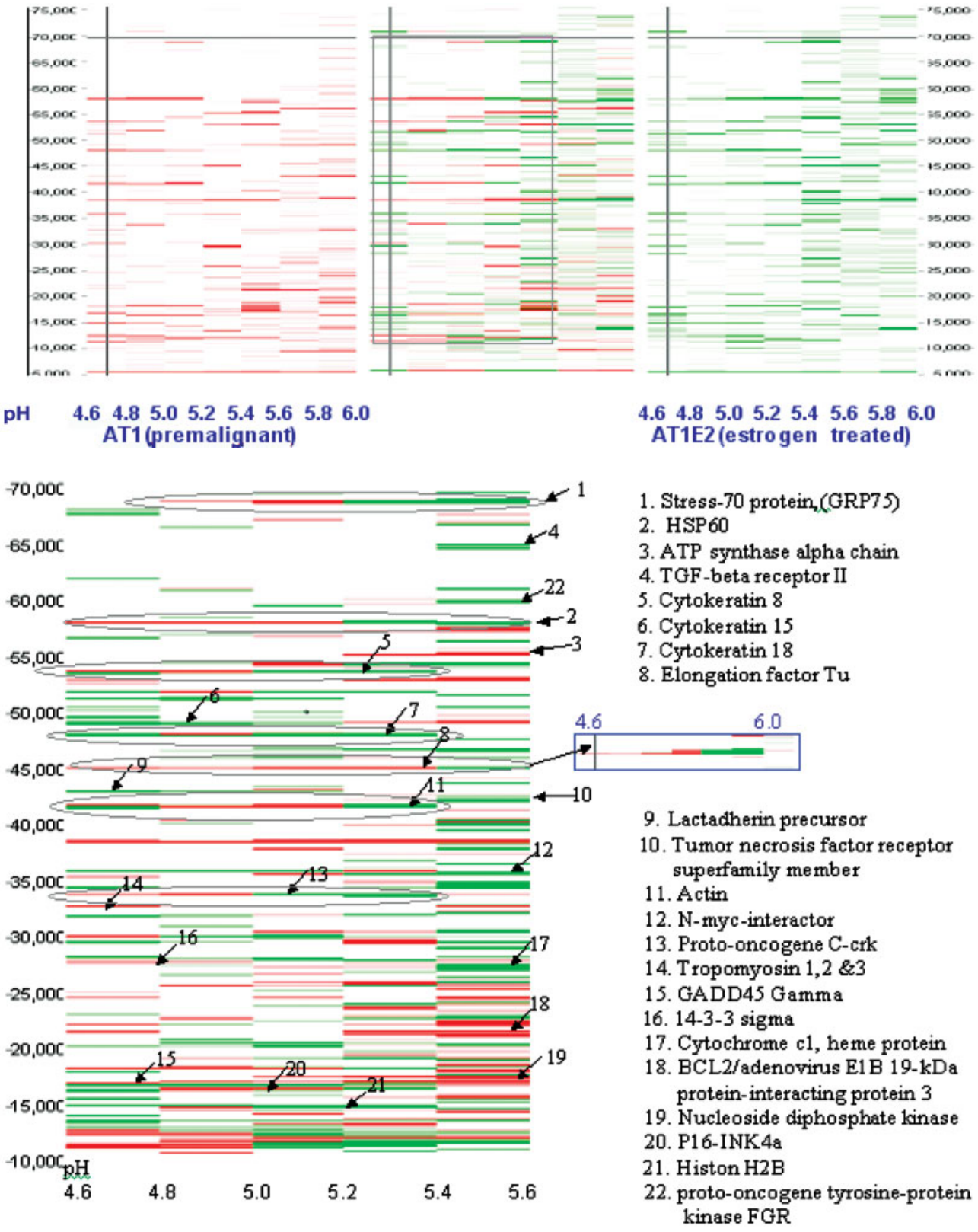

Figure 3. (a) 2-D mass map of cell line MCF10AT1 (left) and MCF10AT1E2 (right) in pH range 4.6–6.0 and M_r range 5–75K. Differential map shown in the middle is generated by point subtraction. (b) Differential map between the two samples was zoomed in to pH 4.6–5.6 and M_r 10–70K. Some mass map-correlated protein IDs were labeled.

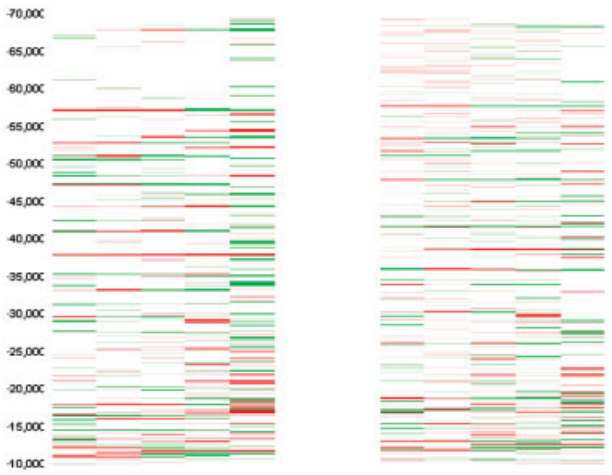

Figure 4. CF-LC-ESI-MS experiments were repeated three times independently and the mass maps were generated. Two differential maps in pH 4.6–5.6 were selected to show the reproducibility.

followed by fraction collection. The collected fractions from RP separation were concentrated, digested, and analyzed by MALDI-TOF-MS or MALDI-TOF/TOF-MS for identification. The protein ID can be correlated to the MW and abundance observed in ESI-TOF-MS using retention time in the RP separation. In this work, ~300 proteins were identified by PMF or sequencing; 120 were detected by ESI-MS and assigned to a band on the mass map.

One disadvantage of PMF is that it biases against proteins with low molecular weight and proteins with low abundance [20], where only limited number of peptides can be detected. This problem can be overcome by MS/MS analysis and the MW of the intact protein obtained from ESI-TOF-MS analysis. Therefore, peptides from proteins with ambiguous identification, unassigned peptides with quality MS signals, and peptides with possible modifications were selected for MALDI-TOF/TOF analysis. In the case of the protein enhancer of rudimentary homolog, a protein M_r 12 259, when analyzed by MALDI-TOF-MS, only two peaks were matched as shown in Fig. 5a, which is insufficient for identification. However, the MS/MS analysis revealed its identity (as shown in Fig. 5b and c) which was confirmed by the MW obtained from the ESI-TOF-MS analysis.

The MW and p*I* of intact proteins acquired in protein profiling using CF-NPS-RP-HPLC-online-ESI-TOF-MS are useful not only in protein ID confirmation but also in revealing PTMs. A difference between the experimental MW/p*I* and the theoretical MW/p*I* is often due to modifications such as truncation and phosphorylation [21]. Some of the proteins identified in this work are categorized in Tables 1–4. Most experimental MW values match well with their corresponding theoretical MW. However, there are some discrepancies in each of the four tables. All the proteins with MW shifts due to truncation are listed in Table 5.

3.5 Differentially expressed proteins after E2 treatment

To identify differentially expressed proteins in these two samples, the mass map of MCF10AT1 and that of MCF10AT1E2 can be overlayed using DeltaVue as shown in Fig. 3b. The red bands are from AT1, and the green bands are from AT1E2. Approximately 40 proteins were detected in each CF fraction by ESI-MS analysis in the mass range 5–75 kDa. Proteins expressed at lower levels might not be observed due to limitations in instrument sensitivity and data processing software. Approximately 70% of the proteins detected are present in both untreated and estrogen-treated cells.

The band intensity indicates the abundance of proteins. However, some high-abundance proteins may appear in more than one CF fraction. On the differential mass map, they are displayed as one wide band covering several pH sections. For example, the theoretical p*I* of cleaved HSP 60 (band 2) has a theoretical p*I* of 5.6 – but it was detected from pH 4.6 to 5.6 – while cytokeratin 18 (band 7) and actin (band 11) have theoretical p*I* of 5.3 and 5.2, respectively; however, they were detected from pH 4.6 to 5.4. To determine the total quantity of these high-abundance proteins, the peak area of each protein in each CF fraction must be summed together to estimate the total amount of the protein in one cell line. In this study, about 120 proteins were selected for quantitation. These proteins, which have high-intensity bands on the massmap, have been detected in at least two experiments and firmly identified.

To obtain reliable quantitation, three duplicate CF-NPS-RP-HPLC-online-ESI-TOF-MS analyses were performed for MCF10AT1 and MCF10AT1E2 cell lysates. The peak area of each of the deconvoluted intact proteins was normalized to that of insulin. The mean and SD of the normalized peak areas obtained from duplicate experiments were calculated for each protein and are shown in Tables 1–3. A SD of 10% can be achieved for high-abundance proteins, while 10–30% SD can be realized for low-abundance proteins. Among the differentially expressed proteins, 70% of them were detected in duplicate experiments. In some cases, proteins are only detected in two duplicate experiments. Therefore, SDs are not available. Alternatively, the average of their normalized protein expressions was used.

3.5.1 Proteins with no obvious changes in expression

Proteins detected in both MCF10AT1 and MCF10AT1E2 lysate are listed in Table 3. These proteins were all firmly identified by PMF, MS/MS, or both. The measured MW of intact proteins all matched well with their corresponding theoretical MW value. As listed, the normalized peak area for each protein in MCF10AT1 and MCF10AT1E2 were shown in separate columns. The change of each protein was calculated by dividing the normalized peak area obtained from MCF10AT1E2 by that obtained from MCF10AT1. Among the 74 proteins listed, actin (alpha, beta, and gamma) and ATP synthase remain unchanged upon estrogen treatment. It is

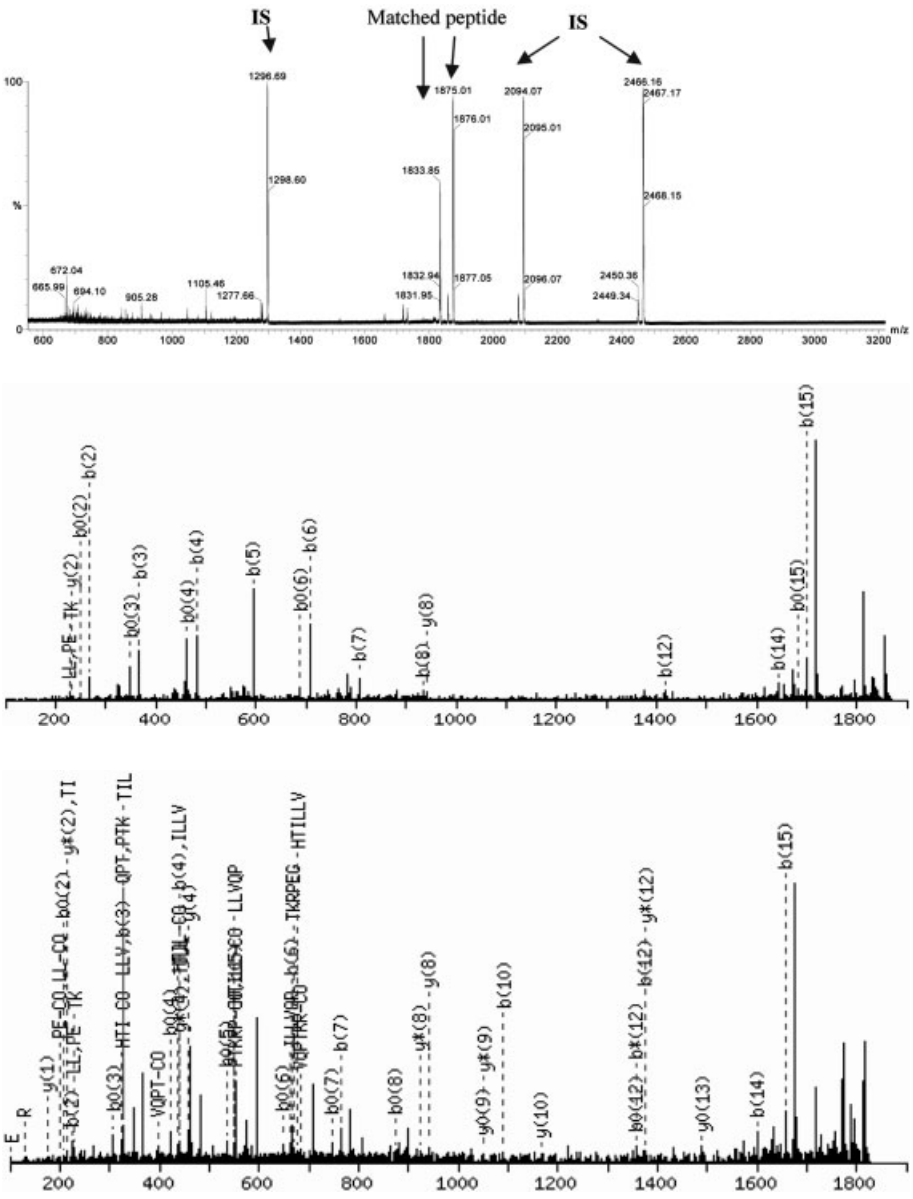

Figure 5. (a) MS spectrum of enhancer of rudimentary homolog (Q14259) after trypsin digestion. Identification is ambiguous because of the low number of peptides detected. Three peptides were added in the matrix as internal standards with *m*/*z* of 1296, 2093, and 2465. (b) MS/MS spectrum of the peptide at *m*/*z* of 1874 was obtained by using MALDI-TOF-TOF. Sequence is SHTILLVQPTKRPEGR + acetyl (*N*-term). (c) MS/MS spectrum of the peptide at *m*/*z* of 1832. Sequence is SHTILLVQPTKRPEGR. Both of these two sequences were confidently identified as Enhancer of rudimentary homolog (Q14259).

worthwhile to point out that actin isoforms were resolved despite their close MW, p*I*, and the low expression of α-actin. Further, many of these proteins are expressed in high levels in both cell lines. Western blot analysis of β-actin levels in whole cell lysates and fractions collected from CF columns from control untreated (panel A) and estrogen-treated (panel B) MCF10AT cells are shown in Fig. 6. The results confirm that the total amounts of this housekeeping protein in unfractionated samples and individual fractions are similar

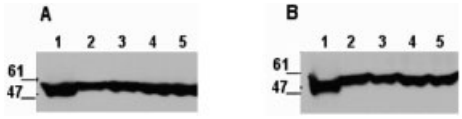

Figure 6. Western blot analysis of β-actin levels in fractions collected from CF columns from control untreated (panel A) and estrogen-treated (panel B) MCF10AT cells. Lane 1, total cell lysate; lane 2, pH 4.6–4.8; lane 3, 4.8–5.0; lane 4, 5.0–5.2; lane 5, 5.2–5.4.

Table 1. Proteins only detected in MCF10AT1E2 by ESI-MS

Acc #	Protein ID	Theo MW/p*I*	Exp MW	Identification Method	Expression In AT1E2[b)]	Change[a)]
O75791	GRB2-related adaptor protein 2	37910/6.4	37901	PMF	0.14 ± 0.03	27 ± 5
Q13976	cGMP-dependent protein kinase 1, alpha isozyme	76365/5.7	76422	PMF	0.13 ± 0.02	27 ± 3
P46108	Proto-oncogene C-crk (P38)	22936/5.2	22940	PMF	0.116 ± 0.015	23 ± 3
O14763	Tumor necrosis factor receptor superfamily member 10B	42202/5.0	42161	PMF	0.120 ± 0.013	23 ± 3
O95881	Thioredoxin-like protein p19 precursor	16426/5.2	16435	PMF	0.09 ± 0.01	18 ± 2
Q15642	Cdc42-interacting protein 4 (Thyoid receptor interacting protein 10)	62592/5.2	62595	PMF	0.06/0.11	17
P13646	Keratin, type I cytoskeletal 13 (Cytokeratin 13) (K13)	49587/4.9	49586	PMF	0.08 ± 0.02	16 ± 3
Q8NBS9	Thioredoxin domain containing protein 5 [Precursor]	47629/5.8	47697	MS/MSPMF	0.08 ± 0.01	15 ± 2
P37173	TGF-beta receptor type II	64540/5.6	64709	PMF	0.05/0.1	15
P09769	Proto-oncogene tyrosine-protein kinase FGR (P55-FGR)	59479/5.4	59509	PMF	0.05/0.08	13
Q9BZD7	Transmembrane gamma-carboxyglutamic acid protein 3	23650/5.3	23650	PMF	0.06 ± 0.02	12 ± 3
P04155	Trefoil factor 1 [Precursor]	9150/4.3	9165	PMF	0.06 ± 0.01	11 ± 2
Q99426	Tubulin-specific chaperone B	27326/5.1	27373	PMF	0.04/0.07	11
P40616	ADP-ribosylation factor-like protein 1	20418/5.6	20410	PMF	0.05 ± 0.02	10 ± 3
P10109	Adrenodoxin, mitochondrial precursor	13561/4.4	13577	PMF	0.05 ± 0.01	10.0 ± 1.9
Q13287	N-myc-interactor (Nmi) (N-myc and STAT interactor)	35117/5.2	35943	PMF	0.03/0.07	10
Q9UQ80	Proliferation-associated protein 2G4	43787/6.1	43814	PMF	0.04/0.06	10
P53667	LIM domain kinase 1	72602/6.5	72850	PMF	0.047 ± 0.008	9 ± 2
P11021	78 kDa glucose-regulated protein precursor (GRP 78)	70478/5.0	70874	MS/MSPMF	0.04 ± 0.01	8 ± 2
Q92843	Apoptosis regulator Bcl-W (Bcl-like 2 protein)	20775/5.4	20706	PMF	0.033 ± 0.007	7 ± 1
P01106	Myc proto-oncogene protein (c-myc)	48804/5.3	48828	PMF	0.008/0.014	7
P24385	G1-S-specific cyclin D1(PRAD1 oncogene)	33729/5.0	33705	PMF	0.03 ± 0.01	5 ± 2
Q13509	Tubulin beta-4 chain (Tubulin beta-III)	50433/4.8	50481	PMF	0.023 ± 0.005	5 ± 1
P08107	Heat shock 70 kDa protein 1 (HSP70.1)	70053/5.5	70086	MS/MSPMF	0.022/0.016	3.8

a) Standard deviation obtained from 3 replicate experiments is indicated. The protein quantity change without STD is the average of two replicate experiments.
The undetected protein level in LC-ESI-TOF MS experiment is assumed as the same with the lowest expression level detected using this instrument (WT1-associated protein in MCF10AT1 cell line). The expression change between detected and undetected expression is calculated on this basis.

b) The mean value of protein expression and the standard deviation obtained from 3 replicate experiments are indicated. For the proteins in which only two values are available, both values are reported.

Table 2. Proteins only detected in MCF10AT1 by ESI-MS

Acc #	Protein ID	Theo MW/p*I*	Exp MW	Identification Method	Expression In AT1[b)]	Change[a)]
P12074	Cytochrome c oxidase polypeptide VIa-liver, mitochondrial [Precursor]	9619/6.4	9619	MS/MSPMF	0.67 ± 0.18	<−50
P55809	Succinyl-CoA:3-ketoacid-coenzyme A transferase 1, mitochondrial precursor	56158/7.1	56157	PMF	0.19 ± 0.01	−38 ± 2
Q12983	BCL2/adenovirus E1B 19-kDa protein-interacting protein 3	21541/6.3	21542	PMF	0.18 ± 0.03	−35 ± 5
P80188	Neutrophil gelatinase-associated lipocalin precursor (NGAL)	22588/9.0	22553	PMF	0.17 ± 0.02	−35 ± 4
O43402	neighbor of COX4	23779/5.9	23775	PMF	0.11 ± 0.02	−23 ± 3
P21266	Glutathione S-transferase Mu 3 (GSTM3-3) (GST class-mu 3) (hGSTM3-3)	26560/5.4	26571	MS/MSPMF	0.09 ± 0.01	−18 ± 2
O95257	Growth arrest and DNA-damage-inducible protein GADD45 gamma	17121/4.3	17070	PMF	0.084 ± 0.014	−17 ± 3
Q13162	Peroxiredoxin	30540/5.9	30545	MS/MSPMF	0.062 ± 0.010	−12 ± 2
P09493	Tropomyosin 1 alpha chain	32709/4.7	32831	MS/MSPMF	0.057 ± 0.009	−11 ± 2
P08727	Keratin, type I cytoskeletal 19 (Cytokeratin 19) (K19) (CK 19)	44106/5.0	44121	PMF	0.04 ± 0.01	−8 ± 2
P14866	Heterogeneous nuclear ribonucleoprotein L (hnRNP L)	60188/6.7	60189	MS/MSPMF	0.042/0.035	−8
P13693	Translationally controlled tumor protein (TCTP) (p23) (Histamine-releasing factor) (HRF)	19596/4.8	19610	MS/MSPMF	0.021/0.032	−5
P27348	14-3-3 protein tau (14-3-3 protein theta) (14-3-3 protein T-cell) (HS1 protein)	27764/4.7	27699	PMF	0.014/0.023	−4

Table 3. Proteins detected in MCF10AT1 and MCF10AT1E2 by ESI-MS

Acc #	Protein ID	Theo MW/p*I*	Exp MW	Identification Method	Expression In AT1[d]	Expression In AT1E2[e]	Change[c]
Q15007	Wilm's tumor 1-associating protein (WT1-associated protein)	17801/5.4	17770	PMF	0.005 ± 0.001	0.12 ± 0.03	23 ± 7
P10599	Thioredoxin (ATL-derived factor) (ADF)	11738/4.8	11742	MS/MSPMF	0.029 ± 0.009	0.52 ± 0.13	19 ± 2
P13645	Keratin, type I cytoskeletal 10 (Cytokeratin 10) (K10) (CK 10)	59519/5.1	59533	MS/MSPMF	0.013 ± 0.002	0.23 ± 0.003	18.5 ± 1.4
Q99757	Thioredoxin, m.p.	18383/8.5	18403	MS/MSPMF	0.14 ± 0.01	2.5 ± 0.5	17 ± 2
Q9UBC7	Galanin-like peptide precursor	10118/6.3	10128	PMF	0.012 ± 0.003	0.18 ± 0.03	15 ± 2
P62502	Epididylmal-specific lipocalin 6 precursor (Lipocalin 5)	18045/4.8	18025	PMF	0.04 ± 0.02	0.52 ± 0.18	14 ± 3
P09382	Galectin-1 (Beta-galactoside-binding lectin L-14-I)	14716/5.3	14711	MS/MSPMF	0.017 ± 0.006	0.2 ± 0.1	11 ± 2
P08729	Keratin, type II cytoskeletal 7 (Cytokeratin 7)	51418/5.5	51460	MS/MSPMF	0.06 ± 0.01	0.66 ± 0.25	11 ± 2
Q14696	Mesoderm development candidate 2	26077/7.6	26060	PMF	0.06 ± 0.03	0.6 ± 0.2	11 ± 2
P09758	Tumor-associated calcium signal transducer 2 precursor	35710/9.3	35691	PMF	0.12 ± 0.07	1.1 ± 0.4	10 ± 3
P01609	IG KAPPA CHAIN V-I REGION SCW	11764/5.7	11793	PMF	0.014 ± 0.007	0.13 ± 0.03	10 ± 3
Q13242	Splicing factor, arginine/serine-rich 9	25542/8.7	25517	MS/MSPMF	0.01 ± 0.002	0.1 ± 0.02	10 ± 2
P38646	Stress-70 protein, mitochondrial precursor (GRP75)	68759/5.4	68763/ 68840	MS/MSPMF	1.2 ± 0.3	11.5 ± 1.5	10 ± 1
O43427	Acidic fibroblast growth factor intracellular binding protein	41878/6.0	42033	MS/MSPMF	0.041 ± 0.006	0.37 ± 0.13	9 ± 2
P49411	Elongation factor Tu, mitochondrial precursor (EF-Tu) (P43)	45045/6.3	45047	MS/MSPMF	0.7 ± 0.3	5.6 ± 1.2	9 ± 2
O00217	NADH-ubiquinone oxidoreductase 23 kDa subunit, mitochondrial precursor	20290/5.1	20291	PMFMS/MS	0.016 ± 0.004	0.15 ± 0.04	9.0 ± 0.2
P19012	Keratin, type I cytoskeletal 15 (Cytokeratin 15)	49168/4.7	49158	MS/MSPMF	0.04 ± 0.01	0.37 ± 0.16	8 ± 1
Q08431	Lactadherin precursor (Milk fat globule-EGF factor 8)	43123/8.5	43088	PMF	0.05 ± 0.02	0.37 ± 0.07	8 ± 2
P11142	Heat shock cognate 71 kDa protein	70899/5.4	70891	MS/MSPMF	0.07 ± 0.01	0.53 ± 0.15	7 ± 1
P04792	HSP27(SRP 27) (Estrogen regulated protein 24 kDa protein)	22783/6.0	22813	PMF	0.017 ± 0.006	0.98 ± 0.02	6 ± 2
P48643	T-complex protein 1, epsilon subunit (TCP-1-epsilon) (CCT-epsilon)	59672/5.5	59643	PMF	0.9 ± 0.2	5 ± 1	5.6 ± 0.1
P35527	Keratin, type I cytoskeletal 9 (Cytokeratin 9) (K9) (CK 9)	61988/5.1	61988	MS/MSPMF	0.016 ± 0.004	0.08 ± 0.02	5.4 ± 0.4
P10644	cAMP-dependent protein kinase type i-alpha regulatory chain	42982/5.3	42983	PMF	0.019/0.024	0.11/0.08	5
P10159	Eukaryotic translation initiation factor 5A (eIF-5A) (eIF-4D)	16832/5.1	16842	PMF	0.22 ± 0.05	0.8 ± 0.2	4 ± 2
P10809	60 kDa heat shock protein, m.p. (HSP-60)	57963/5.2	57966	MS/MSPMF	4.8 ± 1.1	18.8 ± 1.6	4 ± 1
P22626	Heterogeneous nuclear ribonucleoprotein A2/B1	37430/9.0	37431	MS/MSPMF	0.017/0.023	0.09/0.06	4
O14810	Complexin 1 (Synaphin 2)	15030/4.9	15023	PMF	0.9 ± 0.3	2.8 ± 0.4	4 ± 1
P08670	Vimentin	53686/5.1	53649	MS/MSPMF	1.4 ± 0.2	5 ± 1	3.6 ± 0.2
P04899	Guanine nucleotide-binding protein G(i), alpha-2 subunit	40451/5.3	40449	PMF	0.015 ± 0.002	0.05 ± 0.01	3 ± 1
Q9UJC5	SH3 domain-binding glutamic acid-rich-like protein 2	12326/6.3	12351	PMF	0.015 ± 0.003	0.049 ± 0.005	3 ± 1
P05783	Keratin, type I cytoskeletal 18 (Cytokeratin 18) (CK 18)	48058/5.3	48062	MS/MSPMF	1.4 ± 0.3	4.5 ± 0.5	3.2 ± 0.4
Q8N257	Histone H2B type 12	13777/10	13786	MS/MSPMF	0.35 ± 0.02	1.1 ± 0.4	3 ± 1
P22087	Fibrillarin (34 kDa nucleolar scleroderma antigen)	33784/10.2	33791	PMF	0.194 ± 0.006	0.54 ± 0.15	3 ± 1
P08574	Cytochrome c1, heme protein, mitochondrial precursor (Cytochrome c-1)	27352/6.5	27360	MS/MSPMF	0.09 ± 0.01	0.24 ± 0.01	2.6 ± 0.1
P05787	Keratin, type II cytoskeletal 8 (Cytokeratin 8)	53675/5.5	53670	MS/MSPMF	0.25 ± 0.05	0.59 ± 0.03	2.4 ± 0.4
P20827	Ephrin-A1 precursor	23771/6.5	23644	PMF	0.025 ± 0.009	0.06 ± 0.02	2.3 ± 0.5
P46108	Proto-oncogene C-crk (P38) (Adapter molecule crk)	33872/5.5	33847	PMF	0.07 ± 0.02	0.15 ± 0.04	2.3 ± 0.3
P13797	T-plastin	70436/5.5	70365	PMF	0.013 ± 0.003	0.03 ± 0.006	2.3 ± 0.1
P08758	Annexin A5 (Annexin V)	35937/4.9	35921	PMF	0.37 ± 0.04	0.78 ± 0.20	2.1 ± 0.3
P31943	heterogeneous nuclear ribonucleoprotein H	49230/5.9	49215	MS/MSPMF	0.87 ± 0.22	1.7 ± 0.3	2 ± 0.2
P28676	Grancalcin	24010/5.0	24014	PMF	0.011 ± 0.004	0.021 ± 0.004	2 ± 0.3
Q15714	Regulatory protein TSC-22 (TGFB stimulated clone 22 homolog)	15680/5.1	15683	PMF	0.009/0.01	0.016/0.020	1.9
Q9UK45	U6 snRNA-associated- Sm-like protein LSm7	11595/5.1	11601	PMF	0.038 ± 0.002	0.07 ± 0.02	1.8 ± 0.5
P20674	CYTOCHROME C OXIDASE POLYPEPTIDE VA, m.p.	12513/4.9	12509	MS/MSPMF	1.36 ± 0.37	2.26 ± 0.35	1.7 ± 0.2
Q08116	Regulator of G-protein signaling 1 (RGS1)	22475/8.3	22489	PMF	0.056/0.064	0.11/0.08	1.6
P17980	26S protease regulatory subunit 6A (TBP-1)	49204/5.1	49208	PMF	0.66 ± 0.13	1.06 ± 0.38	1.6 ± 0.4
P02304	Histone H4	11367/11	11305	PMF	0.19/0.16	0.3/0.2	1.5
P06576	ATP synthase beta chain, mitochondrial precursor	51769/5.0	51771	MS/MSPMF	1.04 ± 0.33	1.42 ± 0.28	1.4 ± 0.2
O43399	Tumor protein D54 (hD54) (D52-like 2)	22238/5.3	22208	MS/MSPMF	0..028 ± 0.008	0.035 ± 0.007	1.3 ± 0.2
P02570	Actin, cytoplasmic 1 (Beta-actin)	41737/5.3	41720	MS/MSPMF	2.2 ± 0.3	2.87 ± 0.58	1.3 ± 0.1
P02571	Actin, cytoplasmic 2 (Gamma-actin)	41793/5.3	41766	MS/MSPMF	2 ± 0.3	2.65 ± 0.54	1.2 ± 0.1

Table 3. Continued

Acc #	Protein ID	Theo MW/p*I*	Exp MW	Identification Method	Expression In AT1[d)]	Expression In AT1E2[e)]	Change[c)]
P30101	Protein disulfide isomerase A3 precursor (ERp60)	54265/5.6	54264	MS/MSPMF	0.27 ± 0.06	0.33 ± 0.10	1.2 ± 0.1
P05387	60S acidic ribosomal protein P2	11665/4.4	11648	PMF	0.06 ± 0.03	0.07 ± 0.01	1.2 ± 0.3
O75489	NADH-ubiquinone oxidoreductase 30 kDa subunit, m.p.	30242/7.0	30195	PMF	0.20 ± 0.06	0.23 ± 0.03	1.2 ± 0.2
P07355	Annexin A2 (Annexin II) (Lipocortin II)	38604/7.6	38600	MS/MSPMF	21.4 ± 1.9	25.8 ± 3.7	1.2 ± 0.1
P02568	Actin, alpha skeletal muscle (Alpha-actin 1)	42051/5.2	42151	MS/MSPMF	0.04/0.03	0.03/0.04	1.2
O75306	NADH-ubiquinol oxidoreductase 49 kDa subunit, m.p.	52546/7.2	52624	PMF	0.034 ± 0.015	0.04 ± 0.01	1.2 ± 0.2
Q9UJT0	Tublin eplison chain (Epsilon tublin)	52932/6.2	52933	PMF	1.18 ± 0.31	1.33 ± 0.59	1.1 ± 0.2
O75556	Mammaglobin B precursor (Mammaglobin 2)	10884/5.5	10952	MS/MSPMF	0.034 ± 0.018	0.033 ± 0.008	1.1
O75947	ATP synthase D chain, mitochondrial (My032 protein)	18491/5.2	18467	MS/MSPMF	0.13 ± 0.05	0.10 ± 0.03	−1.3 ± 0.1
O00300	Tumor necrosis factor receptor superfamily member 11B precursor	46041/8.7	45967	PMF	0.14 ± 0.04	0.09 ± 0.01	−1.5 ± 0.3
P35080	Profilin II	15046/6.5	15010	PMF	0.14 ± 0.06	0.08 ± 0.02	−1.6 ± 0.3
P24539	ATP synthase B chain, m.p.	24625/9.1	24632	PMF	025 ± 0.07	0.13 ± 0.02	−1.9 ± 0.2
P84103	Splicing factor, arginine/serine-rich 3	19330/11.6	19268	MS/MSPMF	0.063/0.097	0.02/0.03	−3
O75531	Barrier to antointegration factor	10059/5.8	10054	PMF	0.14 ± 0.06	0.046 ± 0.012	−3.0 ± 0.4
Q9Y265	RuvB-like 1 (NMP 238)	50228/6.0	50222	MS/MSPMF	0.44 ± 0.15	0.14 ± 0.04	−3.1 ± 0.3
P07951	Tropomyosin beta chain (Tropomyosin 2)	32851/4.7	32861	PMF	0.021 ± 0.004	0.006 ± 0.002	−3.4
P42771	Cyclin-dependent kinase 4 inhibitor A (CDK4I) (p16-INK4)	16533/5.5	16530	PMF	1.31 ± 0.31	0.33 ± 0.06	−4.0 ± 0.3
P31947	14-3-3 sigma	27774/4.7	27785	MS/MSPMF	0.054 ± 0.017	0.011 ± 0.002	−5 ± 1
Q9NPJ6	Vitamin D3 receptor-interacting protein complex 36 kDa component (DRIP36)	29746/5.0	29747	PMF	2. ± 0.2	0.4 ± 0.1	−6 ± 1
P15531	Nucleoside diphosphate kinase A (NDK A)	17149/5.8	17212	PMF	0.75 ± 0.13	0.14 ± 0.04	−6 ± 1
P25705	ATP synthase alpha chain, mitochondrial precursor	55209/8.3	55206	MS/MSPMF	6.18 ± 0.75	0.32 ± 0.09	−20 ± 3
P08559	Pyruvate dehudrogenase E1 component alpha subunit, m.p.	43296/8.3	43217	MS/MSPMF	1.7 ± 0.2	0.06 ± 0.01	−28 ± 2

c) Protein quantity changes of MCF10AT1E2 *versus* MCF10AT1 between −4 to +4 is in grey.
Standard deviation obtained from 3 replicate experiments is indicated. The protein quantity change without STD is the average of two replicate experiments.

d), e) The mean value of protein expression and the standard deviation obtained from 3 replicate experiments are indicated. For the proteins in which only two values are available, both values are reported.

Table 4. Selected proteins identified by MALDI-MS, not detected in ESI-MS experiment

Acc #	Protein ID	Theo MW/p*I*	Identification Method
Q13541	Eukaryotic translation initiation factor 4E binding protein 1 (4E-BP1)	12580/5.3	PMF
P42772	Cyclin-dependent kinase 4 inhibitor B (p14-INK4b) (p15-INK4b)	14722/6.1	PMF
Q99653	Calcium-binding protein p22 (Calcium-binding protein CHP)	22456/5.0	MS/MSPMF
Q9UMX6	Guanylyl cyclase activating protein 2 (GCAP 2) (Guanylate cyclase activator 1B)	23478/4.7	PMF
Q9HCN8	Stromal Cell-derived factor 2-like protein 1 precursor	23599/6.5	PMF
Q16629	Splicing factor, arginine/serine-rich 7	27367/12	MS/MSPMF
P29312	14-3-3 protein zeta/delta (Protein kinase C inhibitor protein-1)	27745/4.7	PMF
P07226	Tropomyosin alpha 4 chain (Tropomyosin 4) (TM30p1)	28522/4.7	PMF
P42655	14-3-3 protein epsilon (Mitochondrial import stimulation factor L subunit)	29174/4.6	PMF
O43736	integral membrane protein 2A	29742/5.6	PMF
P40222	Hypothetical protein initially thought to be identical with interleukin-14 (IL-14)	30107/6.3	PMF
P47756	F-actin capping protein beta subunit (CapZ beta)	31351/5.4	MS/MSPMF
P30281	G1/S-specific cyclin D3	32520/6.7	PMF
Q15181	Inorganic pyrophosphatase (Pyrophosphate phospho-hydrolase) (PPase)	32660/5.5	MS/MSPMF
P52907	F-actin capping protein alpha-1 subunit (CapZ alpha-1)	32923/5.4	MS/MSPMF
Q01105	Phosphatase 2A inhibitor I2PP2A	33489/4.2	MS/MSPMF
P06493	Cell division control protein 2 homolog (p34 protein kinase)	34096/8.4	PMF
P49888	Estrogen sulfotransferase (Sulfotransferase, estrogen-preferring) (EST-1)	35127/6.2	PMF

Table 4. Continued

Acc #	Protein ID	Theo MW/p*I*	Identification Method
O00214	Galectin-8 (Gal-8) (Prostate carcinoma tumor antigen 1) (PCTA-1)	35539/7.1	PMF
P30519	Heme oxygenase 2 (HO-2)	36033/5.3	PMF
O95755	Ras-related protein Rab-36	36324/7.5	PMF
P04270	Actin, alpha cardiac	42019/5.2	PMF
P48667	Keratin, type II cytoskeletal 6D (Cytokeratin 6D) (CK 6D) (K6D keratin)	42469/5.3	MS/MSPMF
Q16795	NADH-ubiquinone oxidoreductase 39 kDa subunit, m.p.	42510/9.8	PMF
P04637	Cellular tumor antigen p53 (Tumor suppressor p53)	43654/6.3	PMF
P52597	Heterogeneous nuclear ribonucleoprotein F, nucleo-like protein	45541/5.4	MS/MS,PMF
Q12849	G-rich sequence factor-1 (GRSF-1)	48000/5.5	PMF
Q9C075	Keratin, type I cytoskeletal 23 (Cytokeratin 23) (K23) (CK 23)	48068/6.0	MS/MSPMF
Q9UKS6	Protein kinase C and casein kinase substrate in neurons protein 3	48487/5.8	PMF
P35900	Keratin, type I cytoskeletal 20 (Cytokeratin 20) (K20) (CK 20)	48487/5.5	PMF
O75390	Citrate synthase, mitochondrial precursor	51707/8.1	PMF
Q9Y6N5	Sulfide:quinone oxidoreductase, mitochondrial precursor (CGI-44)	49961/9.2	MS/M PMF
P61978	heterogeneous nuclear ribonucleoprotein K	50976/5.2	MS/MSPMF
Q13451	FK506-binding protein 5 (Peptidyl-prolyl cis-trans isomerase) (PPIase)	51213/5.7	MS/MSPMF
P08779	Keratin, type I cytoskeletal 16 (Cytokeratin 16) (K16) (CK 16)	51268/5.0	PMF
P02533	Keratin, type I cytoskeletal 14 (Cytokeratin 14) (K14) (CK 14)	51622/5.1	PMF
P45452	Collagenase 3 precursor (Matrix metalloproteinase-13) (MMP-13)	53820/5.3	PMF
Q9Y512	Sam 50-like protein CGI-51	51963/6.4	MS/MSPMF
P17661	Desmin	53536/5.2	PMF
P07237	Protein disulfide isomerase precursor (PDI) (Prolyl 4-hydroxylase beta subunit)	57117/4.8	PMF
P06239	Proto-oncogene tyrosine-protein kinase LCK (P56-LCK) (LSK)	58001/5.2	PMF
O75363	Breast carcinoma amplified sequence 1 (Novel amplified in breast cancer 1)	61719/5.0	PMF
P13647	Keratin, type II cytoskeletal 5 (Cytokeratin 5) (K5) (CK 5) (58 kDa cytokeratin)	62462/8.1	MS/MSPMF
Q13131	5′-AMP-activated protein kinase, catalytic alpha-1 chain (AMPK alpha-1 chain)	62794/7.3	PMF
O14682	Ectoderm-neural cortex-1 protein (ENC-1) (P53-induced protein 10)	66130/6.4	PMF
P03372	Estrogen receptor (ER) (Estradiol receptor) (ER-alpha)	66216/8.3	PMF
P20700	Lamin B1	66409/5.1	MS/MSPMF
Q03252	Lamin B2	67689/5.3	PMF
P35240	Merlin (Moesin-ezrin-radixin-like protein) (Schwannomin)	69691/6.1	PMF
Q02153	Guanylate cyclase soluble, beta-1 chain (GCS-beta-1)	70515/5.2	PMF
Q9H4B4	Cytokine-inducible serine/threonine-protein kinase (FGF-inducible kinase)	71790/9.3	PMF
O75509	Tumor necrosis factor receptor superfamily member 21 precursor	71846/8.1	PMF
P13667	Protein disulfide isomerase A4 precursor (Protein ERp-72) (ERp72)	72933/5.0	PMF
P02545	Lamin A/C (70 kDa lamin)	74140/6.6	MS/MSPMF
P19338	Nucleolin (Protein C23)	76345/4.6	MS/MSPMF
P23246	Splicing factor, proline-and glutamine-rich	76149/9.4	MS/MSPMF
Q9UQF2	C-jun-amino-terminal kinase interacting protein 1 (JNK-interacting protein 1)	77525/4.9	MS/MSPMF
P57058	Hormonally upregulated neu tumor-associated kinase	79686/9.2	PMF
Q08493	cAMP-specific 3′,5′-cyclic phosphodiesterase 4C (DPDE1) (PDE21)	79902/5.1	PMF
P08238	Heat shock protein HSP 90-beta (HSP 84) (HSP 90)	83265/5.0	PMF
O75330	Hyaluronan mediated motility receptor (Intracellular hyaluronic acid binding protein)	84032/5.6	PMF
Q9Y2X7	ARF GTPase-activating protein GIT1 (G protein-coupled receptor kinase-interactor 1)	84332/6.3	PMF
Q16549	Proprotein convertase subtilisin/kexin type 7 precursor (Proprotein convertase PC7)	86248/5.5	MS/MSPMF
P42224	Signal transducer and activator of transcription 1-alpha/beta	87336/5.7	PMF
Q96CN9	Golgi coiled coil protein 1	87811/5.3	PMF
P22455	Fibroblast growth factor receptor 4 precursor (FGFR-4)	87955/6.4	PMF
P17480	Nucleolar transcription factor 1 (Upstream binding factor 1) (UBF-1)	89407/5.6	PMF
Q8WXW3	Progesterone-induced blocking factor 1	89774/5.8	PMF
O95294	RasGAP-activating-like protein 1	89998/6.1	PMF
O15394	Neural cell adhesion molecule 2 precursor (N-CAM2)	92933/5.8	PMF
P34932	HEAT SHOCK 70 KDA PROTEIN 4 (HEAT SHOCK 70-RELATED PROTEIN APG-2)	94301/5.2	PMF
P16591	Proto-oncogene tyrosine-protein kinase FER (p94-FER) (c-FER)	94625/6.7	PMF
P45974	Ubiquitin carboxyl-terminal hydrolase 5 (Ubiquitin thiolesterase 5)	95787/4.9	PMF
Q92598	Heat-shock protein 105 kDa	96866/5.3	PMF
P16144	Integrin beta-4 precursor (GP 150) (CD 104 antigen)	202023/5.7	MS/MSPMF

Table 5. Proteins detected as truncated form by ESI-MS

Acc #	Protein ID	Theo MW/p*I*	Exp MW	Cleaved Form	Cleaved AA
P08574	Cytochrome c1, heme protein, mitochondrial precursor	35390/9.1	27360	27352/6.5	1~84
O95881	Thioredoxin-like protein p19 precursor	19206/5.2	16435	16426/5.2	1~26
O00217	NADH-ubiquinone oxidoreductase 23 kDa subunit, mitochondrial precursor	23705/6.0	20291	20290/5.1	1~34
O14763	Tumor necrosis factor receptor superfamily member 10B precursor	47851/5.4	42161	42202/5.0	1~55
P11021	78 kDa glucose-regulated protein precursor	72334/5.1	70507	70478/5.0	1~18
Q9BZD7	Transmembrane gamma-carboxyglutamic acid protein 3 precursor	25848/5.8	23650	23650/5.3	1~19
P10109	Adrenodoxin, mitochondrial precursor	19393/5.5	13577	13561/4.4	1~60
P12074	Cytochrome c oxidase polypeptide VIa-liver, m.p.	12155/9.3	9619	9619/6.4	1~24
P38646	Stress-70 protein, mitochondrial precursor	73681/5.9	68763	68759/5.4	1~46
Q9UBC7	Galanin-like peptide precursor	12545/5.9	10128	10118/6.3	1~24
P49411	Elongation factor Tu, mitochondrial precursor (EF-Tu) (P43)	49542/7.3	45047	45045/6.3	1~43
P10809	60 kDa heat shock protein, m.p. (HSP-60)	61055/5.7	57966	57963/5.2	1~26
P20674	CYTOCHROME C OXIDASE POLYPEPTIDE VA, m.p.	16774/6.3	12509	12513/4.9	1~41
P06576	ATP synthase beta chain, mitochondrial precursor	56560/5.3	51771	51769/5.0	1~47
P30101	Protein disulfide isomerase A3 precursor (ERp60)	56783/6.0	54264	54265/5.6	1~24
P24539	ATP synthase B chain, m.p.	28909/9.4	24632	24625/9.1	1~42
P25705	ATP synthase alpha chain, mitochondrial precursor	59751/9.2	55210	55209/8.3	1~43

between the two samples. Annexin A2 is a reported marker protein [22], but its expression level remain unchanged upon estrogen treatment. The SD of the changes is within 20%. Actually, the same SD window can be applied to proteins with low abundance such as NADH-ubiqinol oxidoreductase 49 kDa subunit.

3.5.2 Proteins with changes in expression

In Table 3, many proteins have changes greater than two-fold. Among them, Hsp60, CK8, CK15, CK7, CK18 are well-documented marker proteins in breast cancer [23–26]. They are mostly structural proteins that have no relation with signal pathways. Moreover, they are typically expressed at high levels, which is true in MCF10AT1 and MCF10AT1E2. Therefore, these proteins are of limited interest.

In addition to accurate mass and accurate p*I*, another improvement on the 2-D mass map generated by the CF-NPS-RP-HPLC-online-ESI-TOF-MS analysis is quantitation. As described previously, the abundance of a protein is measured by the peak area in the deconvoluted MS spectrum. MS is a mass specific detector that can resolve and quantify multiple proteins in a single detection. Therefore, coeluting proteins, that are difficult to quantify in 2-D gel-based techniques, can be resolved and quantified by the MS-based liquid 2-D protein profiling method. This allows the quantification of low-abundance proteins. To minimize the determination of false changes, all proteins with changes higher than 4 are considered changed. In Table 3, WT1 (Q15007) and thioredoxin (Q99757) are both weakly expressed in MCF10AT1 cells, but their expression is significantly elevated upon estrogen treatment. It is not surprising since WT1 protein (Q15007) is correlated with the proliferation of breast cancer cells and it functions partially as an oncogene by stimulating the expression of c-myc proto-oncogene [27, 28]. It should be pointed out that MCF10AT1E2 cells are premalignant. The expression of WT1 protein after the estrogen treatment could be an upstream event that induces the progression of breast cancer. Thioredoxin (Q99757) is one of the major proteins regulating intracellular redox metabolism and it is activated in response to oxidative stress. Studies have shown that the expression of thioredoxin mRNA can be induced by estrogen [29]. The direct evidence of the increased expression of thioredoxin upon estrogen exposure has never been reported. HSP27 (P04792), also referred to as the estrogen-regulated 24K protein, is six times more highly expressed in the estrogen-treated MCF10AT1 cells. Its expression is physiologically related to cell growth and differentiation. Our observation agrees with the suggestion that the differential expression of HSP27 is an important determinant in initiating or promoting a population of human mammary cancers [30].

As shown in Table 3, the expression of stress-70 protein (P38646, GRP75) was elevated ten times upon estrogen treatment. Interestingly, the Western blot analysis of GRP75 protein in total cell lysates of MCF10AT1 and MCF10AT1E2 cells suggests a slight increase (Fig. 7A). However, the analysis of the same protein using Western blot for fractions eluted from the CF column from MCF10AT1 (Fig. 7B) and MCF10AT1E2 (Fig. 7C) cell lysate indicated that approximately eight-fold higher level of GRP75 is detected in estrogen-treated MCF10AT1 cells as compared to the control following fractionation. The results suggest that additional isoforms of GRP75 protein may be present outside the pH range analyzed. It should be noted that a significant portion of GRP75 in MCF10AT1E2 cells appears as a doublet band (compare lanes 2 and 3 in Fig. 7B and C) indicating estrogen-induced PTM, possibly phosphorylation since it predominantly elutes

Figure 7. Western blot analysis of Grp75 protein in total cell lysates of MCF10AT1 (untreated) and MCF10AT1E2 (estrogen-treated) cells (panel A), and of fractions eluted from CF column from untreated (panel B) and estrogen-treated (panel C) MCF10AT1 cells. Lane 1, pH 5.0–4.8; lane 2, 5.0–5.2; lane 3, 5.2–5.4; lane 4, 5.4–5.6; lane 5, 5.6–5.8; lane 6, 5.8–6.0.

at lower pH (5.2–5.0), and a peak at 68 840 Da, ~80 Da higher than the theoretical MW of 68 763 Da, was observed in the estrogen-treated sample. The result revealed the limitation of the traditional 1-D gel separation and supported the advantage of the high-resolution 2-D liquid separation in analysis of complex samples such as whole cell lysate. It should be also noted that GRP75 was shown in 4.8–5.2 fractions in the AT1 map and in 5.0–5.6 in the AT1E2 map as indicated in Fig. 3b. There might be a pH shift due to temperature difference or calibration/electrode difference in separate experiments. It is thus possible that individual isoforms may be identified in adjacent pH fractions in separate experiments.

Some proteins can only be detected in one cell line by ESI-TOF-MS. Those detected only in MCF10AT1E2 cells are shown in Table 1, and those detected only in MCF10AT1 are shown in Table 2. In order to estimate the changes of these proteins, the normalized peak area of each protein is divided by that of the WT1 protein (Q15007), which is the lowest abundant protein detected using the liquid 2-D protein profiling method. As shown in Table 1, GRB2-related adaptor protein 2 (O75791), trefoil factor 1 (P04155), LIM domain kinase 1 (P53667), apoptosis regulator Bcl-W (Q92843), G1-S-specific cyclin D1 (P24385), and c-myc (P01106) can only be observed in MCF10AT1E2 cells, which indicates the up-regulation of these proteins after estrogen treatement. GRB2-related adaptor protein 2 couples tyrosine kinase to the ras signaling pathway [31]. Since the MCF10AT1 cell line is derived from MCF10A cells by c-Ha-ras gene transfection, the observation of GRB2-related adaptor protein indicates the activation of the ras signaling pathway. In addition to the GRB2-related adaptor protein, other proteins observed and involved in the ras signaling pathway include mortalin (P38646, Table 3) [32] and galectin 1 (P09382, Table 3) which have been elevated by 17- and 11-fold, respectively. The increase of galectin 1 mediates ras membrane anchorage and cell transformation [33], and enhances ras signal transduction response to EGF [34]. LIM domain kinase 1 (P53667) is a critical regulator of actin dynamics. It plays a regulatory role in tumor cell invasion. The significant elevation of this protein in MCF10AT1E2 is unexpected since MCF10AT1E2 is still premalignant and noninvasive. Apoptosis regulator Bcl-W (Q92843) promotes cell survival. Increased expression of this protein suggests the decrease of apoptotic signaling. G1-S-specific cyclin D1 (P24385) and c-myc (P01106) are two other proteins which are up-regulated and play an important role in signal pathways. They were identified in both cell lines by MALDI-MS, but their intact form in MCF10AT1 is below the detection limit of the method. Cyclin D1 is essential for the control of the cell cycle at the G1/S transition. The results agree with the positive correlation of the mRNA study of cycline D1 with the ER [35]. On the other hand, c-myc participates in the regulation of gene transcription. C-myc expression may be an important step in the estrogen-induced proliferation of human breast cancer cells [36].

Other proteins were down-regulated upon estrogen treatment. Among them, 14-3-3 protein tau (P27348, Table 2) can only be detected in MCF10AT1, while another protein in the 14-3-3 family, 14-3-3 protein sigma (P31947), is down-regulated by five-fold after estrogen treatment. The 14-3-3 family is a highly conserved family of proteins that play a role in the regulation of signal transduction pathways implicated in the control of cell proliferation, differentiation, and survival. Other important down-regulated proteins include BCL2 protein (Q12983, Table 2), growth arrest and DNA-damage-inducible protein GADD45 gamma (O95257, Table 2), tropomyosin 1 alpha chain (P09493, Table 2), and tropomyosin beta chain (P07951, Table 3).

3.5.3 Proteins with no quantitative information

Proteins remain in solution during the CF and the RP separation. This feature significantly improves the recovery of tryptic peptides, which allows ~300 proteins identified for MCF10AT1 and MCF10AT1E2 in pH 4.6–6.0. In this study, many bands corresponding to proteins identified by MALDI-TOF-MS or MALDI-TOF/TOF-MS analysis are missed on the 2-D mass map. Selected proteins of interest are summarized on Table 4. Around 50% of these proteins have theoretical M_r greater than 60K, where the performance of our current ESI-TOF-MS instrument has limited sensitivity. Some modifications, such as phosphorylation and glycosylation, will decrease the ionization efficiency of proteins. Therefore, heavily modified proteins very likely remain undetected upon ESI-TOF-MS analysis. As a result, the proteins in Table 4 are not quantified although there are some interesting and important proteins such as G1/S-specific cyclin D3 (P30281), EST-1 (P49888), ras-related protein Rab-36 (O95755), cellular tumor antigen p53 (P04637), breast carcinoma amplified sequence 1 (O75363), and ER (P03372).

4 Concluding remarks

In this study, a protein profiling method based on CF-NPS-RP-HPLC-online-ESI-TOF-MS analysis was developed. 2-D mass maps in the pH range 4.6–6.0 were generated with good correlation to theoretical values for intact proteins. The application of the method to MCF10AT1 and the estrogen-

treated MCF10AT1E2 enables the quantification of 120 proteins in mass range 5–75 kDa, where ~40 proteins were found to be up-regulated (>four-fold) upon estrogen treatment while 17 proteins were down-regulated (>four-fold). The remaining proteins were found unchanged. There are some over-expressed proteins which might be essential in the estrogen regulation mechanism such as WT-1 protein, thioredoxin, and Hsp27. The up-regulated proteins include G1-S-specific cyclin and c-myc, which play an important role in signal pathways as well as apoptosis regulator Bcl-W and LIMK which have characteristics consistent with the development of a malignant phenotype. In addition, some altered proteins have a role in the ras pathway such as GRB2-related adaptor protein, Mortalin. There are also some interesting proteins found to be down-regulated including 14-3-3 sigma and tropomyosin 1 alpha chain. Further studies on these proteins will reveal the mechanism of breast cancer progression and the effect of estrogen. Our studies suggest the diverse signal network and cell regulatory pathways through which E2 operates to alter the proliferation and phenotype of high-risk premalignant breast cells.

We gratefully acknowledge support of this work by the National Cancer Institute under grants R21CA83808 (DML, FRM), R01CA90503 (FRM, DML), as well as the National Institutes of Health under RO1GM49500 (DML). We also acknowledge the National Science Foundation under grant DBI 99874 for funding of the MALDI-TOF-MS instrument used in this work.

5 References

[1] Polyak, K., *Biochim. Biophys. Acta* 2001, *1552*, 1–13.

[2] American Cancer Society, *Cancer Facts and Figures 2004*, http://www.cancer.org/downloads/stt/caff_finalpwsecured.pdf.

[3] Russo, I. H., Russo, J., *J. Mammary Gland Biol. Neoplasia* 1998, *3*, 49–61.

[4] Anderson, E., Clarke, R. B., Howell, A., *J. Mammary Gland Biol. Neoplasia* 1998, *3*, 23–35.

[5] Hondermarck, H., Dolle, L., El Yazidi-Belkoura, I., Vercoutter-Edouart, A. S. *et al.*, *J. Mammary Gland Biol. Neoplasia* 2002, *7*, 395–405.

[6] Souchelnytskyi, S., *J. Mammary Gland Biol. Neoplasia* 2002, *7*, 359–371.

[7] Anderson, L., Seilhamer, J., *Electrophoresis* 1997, *18*, 533–537.

[8] Aebersold, R., Mann, M., *Nature* 2003, *422*, 198–207.

[9] Hondermarck, H., Vercoutter-Edouart, A. S., Revillion, F., Lemoine, J. *et al.*, *Proteomics* 2001, *1*, 1216–1232.

[10] Osborne, C. K., Hobbs, K., Clark, G. M., *Cancer Res.* 1985, *45*, 584–590.

[11] Soule, H. D., Vazguez, J., Long, A., Albert, S., Brennan, M., *J. Natl. Cancer Inst.* 1973, *51*, 1409–1416.

[12] Lee, G. S., Ryu, K. S., Rha, J. G., Kim, S. P. *et al.*, *J. Obstet. Gynaecol. Res.* 2002, *28*, 141–148.

[13] Lubman, D. M., Kachman, M. T., Wang, H., Gong, S. *et al.*, *J. Chromatogr. B Analyt. Technol. Biomed. Life Sci.* 2002, *782*, 183–196.

[14] Chong, B. E., Hamler, R. L., Lubman, D. M., Ethier, S. P. *et al.*, *Anal. Chem.* 2001, *73*, 1219–1227.

[15] Miller, F. R., *J. Mammary Gland Biol. Neoplasia* 2000, *5*, 379–391.

[16] Dawson, P. J., Wolman, S. R., Tait, L., Heppner, G. H., Miller, F. R., *Am. J. Pathol.* 1996, *148*, 313–319.

[17] Bradford, M. M., *Anal. Biochem.* 1976, *72*, 248–254.

[18] Shekhar, M. P., Nangia-Makker, P., Wolman, S. R., Tait, L. *et al.*, *Am. J. Pathol.* 1998, *152*, 1129–1132.

[19] Shekhar, P. V., Chen, M. L., Werdell, J., Heppner, G. H. *et al.*, *Int. J. Oncol.* 1998, *13*, 907–915.

[20] Zhu, K., Miller, F. R., Barder, T. J., Lubman, D. M., *J. Mass Spectrom.* 2004, *39*, 770–780.

[21] Zhu, K., Zhao, J., Lubman, D. M., Miller, F. R., Barder, T. J., *Anal. Chem.* 2005, *77*, 2745–2755.

[22] Hamler, R. L., Zhu, K., Buchanan, N. S., Kreunin, P. *et al.*, *Proteomics* 2004, *4*, 562–577.

[23] Trask, D. K., Band, V., Zajchowski, D. A., Yaswen, P. *et al.*, *Proc. Natl. Acad. Sci. USA* 1990, *87*, 2319–2323.

[24] Sarto, C., Binz, P. A., Mocarelli, P., *Electrophoresis* 2000, *21*, 1218–1226.

[25] Cappello, F., Bellafiore, M., Palma, A., David, S. *et al.*, *Eur. J. Histochem.* 2003, *47*, 105–110.

[26] Franzen, B., Linder, S., Alaiya, A. A., Eriksson, E. *et al.*, *Br. J. Cancer* 1996, *74*, 1632–1638.

[27] Zapata-Benavides, P., Tuna, M., Lopez-Berestein, G., Tari, A. M., *Biochem. Biophys. Res. Commun.* 2002, *295*, 784–790.

[28] Han, Y., San-Marina, S., Liu, J., Minden, M. D., *Oncogene* 2004, *23*, 6933–6941.

[29] Maruyama, T., Sachi, Y., Furuke, K., Kitaoka, Y. *et al.*, *J. Endocrinol.* 1999, *140*, 365–372.

[30] O'Neill, P. A., Shaaban, A. M., West, C. R., Dodson, A. *et al.*, *Br. J. Cancer* 2004, *90*, 182–188.

[31] Feng, G. S., Ouyang, Y. B., Hu, D. P., Shi, Z. Q. *et al.*, *J. Biol. Chem.* 1996, *271*, 12129–12132.

[32] Wadhwa, R., Yaguchi, T., Hasan, M. K., Taira, K., Kaul, S. C., *Biochem. Biophys. Res. Commun.* 2003, *302*, 735–742.

[33] Paz, A., Haklai, R., Elad-Sfadia, G., Ballan, E., Kloog, Y., *Oncogene* 2001, *20*, 7486–7493.

[34] Elad-Sfadia, G., Haklai, R., Ballan, E., Gabius, H. J., Kloog, Y., *J. Biol. Chem.* 2002, *277*, 37169–37175.

[35] Hui, R., Cornish, A. L., McClelland, R. A., Robertson, J. F. *et al.*, *Clin. Cancer Res.* 1996, *2*, 923–928.

[36] Dubik, D., Dembinski, T. C., Shiu, R. P., *Cancer Res.* 1987, *47*, 6517–6521.

